Noise-driven cooperative dynamics between vegetation and topography in riparian zones

AGU PUBLICATIONS

Geophysical Research Letters

RESEARCH LETTER
10.1002/2015GL065688

Key Points:
- A stochastic model elucidates how random variations of water stage shape riparian transects
- A key feature of the model is to consider that vegetation alters the plot topography
- Vegetation modifies the topography for creating conditions more suitable to its survival

Supporting Information:
- Supporting Information S1

Correspondence to:
R. Vesipa,
riccardo.vesipa@polito.it

Citation:
Vesipa, R., C. Camporeale, and L. Ridolfi (2015), Noise-driven cooperative dynamics between vegetation and topography in riparian zones, *Geophys. Res. Lett.*, *42*, doi:10.1002/2015GL065688.

Received 6 AUG 2015
Accepted 21 SEP 2015
Accepted article online 25 SEP 2015

Noise-driven cooperative dynamics between vegetation and topography in riparian zones

R. Vesipa[1], C. Camporeale[1], and L. Ridolfi[1]

[1]Department of Environment, Land and Infrastructure Engineering, Politecnico di Torino, Turin, Italy

Abstract Riparian ecosystems exhibit complex biotic and abiotic dynamics, where the triad vegetation-sediments-stream determines the ecogeomorphological features of the river landscape. Random fluctuations of the water stage are a key trait of this triad, and a number of behaviors of the fluvial environment can be understood only taking into consideration the role of noise. In order to elucidate how randomness shape riparian transects, a stochastic model that takes into account the main links between vegetation, sediments, and the stream is adopted, emphasizing the capability of vegetation to alter the plot topography. A minimalistic approach is pursued, and the probability density function of vegetation biomass is analytically evaluated in any transect plot. This probability density function strongly depends on the vegetation-topography feedback. We demonstrate how the vegetation-induced modifications of the bed topography create more suitable conditions for the survival of vegetation in a stochastically dominated environment.

1. Introduction

The riparian zone is a transitional area located between freshwater bodies and upland communities that is highly affected by the fluvial hydrological regime [*Naiman et al.*, 2005]. It is a fragile environment that hosts ecomorphological processes with profound environmental and ecological significance. Riparian wetlands are the habitat of a great variety of animal species [*Malanson*, 1993] and act as protection for the bankline from erosion and collapse [*Docker and Hubble*, 2008]. Furthermore, the alternation between wet and dry conditions catalyzes a range of biological and chemical reactions, which decrease the availability of nutrients and the toxicity of contaminants [*Craig et al.*, 2008].

A biogeomorphologic fundamental role is played by the riparian vegetation, i.e., the plant community that develops near rivers and that is influenced by water table variations and the occurrence of flooding [*Tockner et al.*, 2000]. Riparian vegetation is an active element which is able to modify river morphology in order to maximize site colonization and growth, by interacting with sediment transport. Accordingly, riparian vegetation behaves as a river engineer (in the sense of *Jones et al.* [1994]). For instance, in the Paleozoic, the river landscape evolution was impacted tremendously by the development of riparian species, in terms of braiding-meandering transition [*Gibling and Davies*, 2012]. Another interesting case has been documented in Yellowstone Park where the reintroduction of wolves activated a trophic cascade down to the riparian vegetation which eventually affected the overall physical geography of the park [*Beschta and Ripple*, 2006]. These phenomena provide the evidence that the riparian ecotone is a dynamic interface, where ecological and morphological timescales are comparable and the interactions between biotic and abiotic processes are maximized. An emblematic example is provided by the Tagliamento river (see Figure 1), a braided river in the northeast Italy that has stimulated a great deal of research, due to its almost pristine conditions. In the 1.5 km long Flagogna reach, the strong flood of June 2003 reduced the biomass of the riparian vegetation (Figure 1a). Such biomass loss was partially recovered after 9 years (Figure 1b).

Today, a major challenge is to find realistic but at the same time simple models that account for the most significant interrelated processes that are involved in this systems [*Camporeale et al.*, 2013]. This is the aim of the present work.

A number of complex phenomena occur in the interplay between water stream, sediments, and vegetation. (i) The flow field is affected by the riparian vegetation that, in turn, alters the sediment mobilization, transport, and deposition [*Bennett et al.*, 2008; *Ishikawa et al.*, 2003]. (ii) Large woody debris protect and reinforce river banks and floodplains, creating landforms on which new vegetation can grow [*Gurnell et al.*, 2005, 2012].

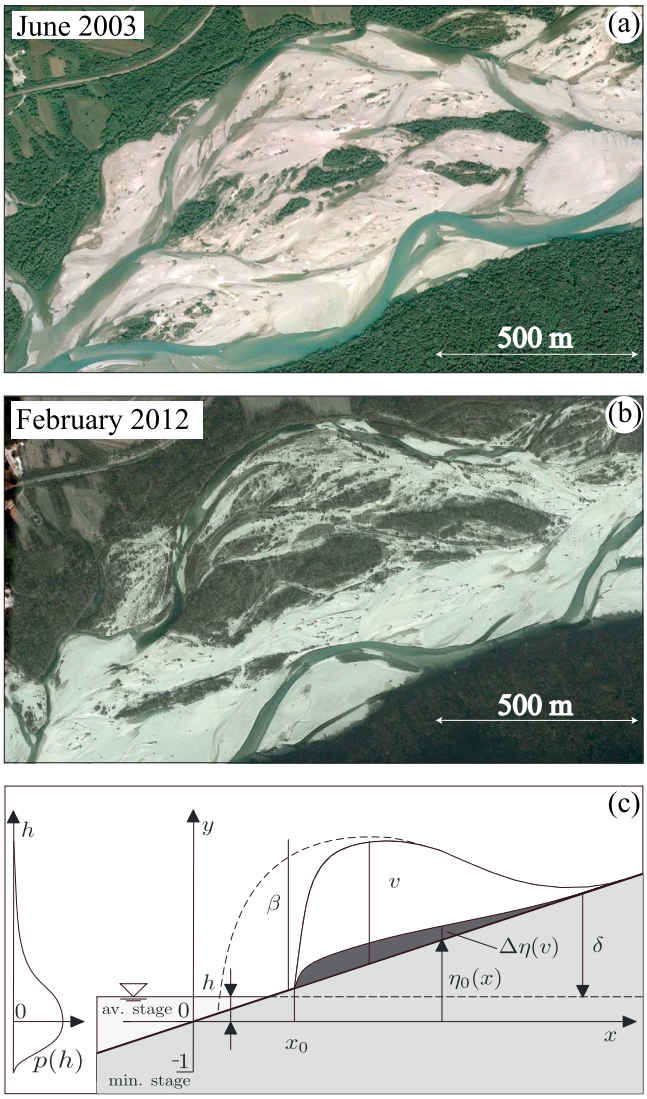

Figure 1. (a, b) The Flagogna reach in June 2003 and February 2012, respectively. (c) Sketch of a riparian plot. The bed elevation before any vegetation colonization (thick black line), the sediment deposition induced by the vegetation (dark grey zone), the plot-specific dimensionless biomass (thin black line), and the plot-specific mean carrying capacity (dashed line) are shown.

(iii) Roots impact the soil properties (resistance to erosion, moisture content, etc.); (iv) Unsteady river flows provide water and nutrients to vegetation, convey sediments (building new sites for vegetation), and exert an hydrological constraint on the root development [*Pasquale et al.*, 2012]. (v) Finally, overflows remove vegetation by erosion and uprooting.

A fundamental result of the above scenario is that riparian vegetation increases the bed elevation in order to create favorable conditions to its development [*Gurnell*, 2014], when forced stochastically by river flows. This in turn leads to a stabilization of the vegetated landforms, which are protected from further erosions. Therefore, flow stocasticity drives a cooperative dynamics between vegetation and topography. This sort of cooperation is not exclusive to riparian vegetation but has been also observed in other biomorphodynamic contexts, such as salt marshes [*Marani et al.*, 2013].

Basically, river ecomorphodynamics are regulated by a triad of key interrelated processes: vegetation dynamics, sediment dynamics, and flow unsteadiness. Most of the existing models account no more than two of these elements, as reviewed in *Corenblit et al.* [2007]; *Camporeale et al.* [2013]. Several studies have

demonstrated that changes of the probabilistic structure of river water stages (by river regulations or climate changes) may induce catastrophic damage on the vegetation, such as reduction of biomass and changes of dominant species [*Shafroth et al.*, 2002; *Tealdi et al.*, 2011; *Doulatyari et al.*, 2014]. Past theoretical works [*Camporeale and Ridolfi*, 2006; *Muneepeerakul et al.*, 2007] have modeled the key role of stochasticity in generating complex behaviors in the spatiotemporal dynamics of vegetation on nonevolving topography, such as noise-induced stability and bimodality [*Camporeale and Ridolfi*, 2007]. The morphological changes induced by static vegetation patches (i.e., without considering vegetation dynamics) have been numerically modeled for gravel bed rivers [*Wu et al.*, 2005; *Crosato and Saleh*, 2011] and sand rivers [*Nicholas et al.*, 2013]. Recently, the dynamics of vegetation patches have been also considered [*Bertoldi et al.*, 2014; *Crouzy et al.*, 2015].

Analyses performed so far were based on complex physical experiments or detailed numerical simulations. A shortcoming of these studies is that considering properly the key role of river stage stochasticity in combination with sediment transport and vegetation dynamics is very demanding from a computational point of view. This task can more readily be achieved by adopting a minimalistic stochastic model. This model can describe the essential physical and the biological processes in a simple but realistic way and can be analytically solved. This approach is particularly efficient for understanding how flow randomness impacts riparian ecomorphodynamics.

The first stochastic models for riparian vegetation [*Camporeale and Ridolfi*, 2006; *Muneepeerakul et al.*, 2007; *Camporeale and Ridolfi*, 2007; *Tealdi et al.*, 2011] provided key insight about vegetation dynamics but disregarded the effect of the vegetation-induced morphological alteration of the river transect (i.e., the transect was considered fixed). By contrast, in this work the vegetation-topography feedback is considered, in order to quantify the role of the vegetation on the biomorphology of riparian transects. An assessment is made of how the vegetation-induced bed elevation affects the total biomass and its distribution along the river transect. The fundamental feedback between the system variable (i.e., vegetation biomass) and topography is considered in the formulation, giving rise to an interesting example of a state-dependent stochastic process. This class of processes is widespread in nature and has been recognized to contribute to the survival of vegetation in hostile environments [*D'Odorico et al.*, 2007; *Ridolfi et al.*, 2011].

2. Physical Processes and Stochastic Model

A generic riparian plot experiences random sequences of flooding and exposing periods induced by the river flow variability. As a consequence, vegetation alternates between decay and growth phases. During high water stages, the submerged vegetation suffers from anoxia, burial, and uprooting, and the plot biomass is reduced. The decay rate depends on the local water depth in the plot. In fact, it controls the shear stresses induced by the stream that, in turn, induce vegetation decline. When low water stages occur, the plot is exposed, and the (phreatophyte) vegetation biomass dynamics is dictated by the depth of the phreatic surface, δ (see Figure 1c). If δ falls in a species-specific range, $[\delta_1, \delta_2]$, plant water uptake occurs in an optimal way, and the vegetation grows. Differently, when $\delta < \delta_1 \quad (\delta > \delta_2)$ the root anoxia (weak capillary fringe) prevents the optimal water uptake. Mathematically speaking, $\delta_{1,2} = \delta_{\mathrm{opt}} \mp \sqrt{1/a}$, where δ_{opt} is the phreatic surface depth that allows the optimal plant growth [*Kozlowski*, 1984; *Naumburg et al.*, 2005] and a is a parameter that describes the sensitivity of the vegetation to a departure of the water table depth from δ_{opt}. Riparian soil permeability is typically high, and the water table position is assumed equal to the river water stage.

In a riparian plot, the durations of flooding and exposing periods, the magnitude of inundation, and the depth of the phreatic surface are random variables. They depend on the probabilistic structure of the river water stage (probability density function and autocorrelation function) and on the topographic elevation of the plot. It follows that the riparian vegetation exhibits a stochastic growth/decay dynamics forced by random fluctuations of the river water stage. Previous studies [*Camporeale and Ridolfi*, 2006, 2007; *Doulatyari et al.*, 2014] demonstrated that the spatiotemporal pattern of vegetation along the river transect is highly dependent on the stochastic variations of the water stage. However, transect topography was assumed fixed, and the interactions between vegetation and morphology were disregarded. Our purpose is to fill this gap.

Field experiments have demonstrated that the vegetation strongly influences the elevation of riparian plots [*Hickin*, 1984]. This influence is induced by a number of mechanisms, such as the trapping of water- and wind-transported sediment particles, the production of organic soil, and the stabilization of the soil surface [*Abbe and Montgomery*, 2003]. As a result, a correlation develops between vegetation biomass and plot

elevation [*Steiger et al.*, 2001]. This link can be modeled through a phenomenological dimensionless relationship of the form

$$\eta = \eta_0 + \Delta\eta(v) = \eta_0 + r \cdot v, \tag{1}$$

where the total bed elevation, η, is given by two terms: the plot elevation, η_0, in bare soil conditions, and the bed elevation increment, $\Delta\eta(v)$, induced by the riparian vegetation biomass, v. In (1), $r > 0$ is an empirical coefficient in the range [0, 0.5]. As the vegetation-induced mechanisms responsible of topographic alterations are not generally affected by the position along the transect, the coefficient r is assumed constant. The extension to the case $r = r(x)$ is straightforward. The elevation is made dimensionless as $\eta = (\eta^* - \bar{h}^*)/\bar{h}^*$, where $\bar{h}^*$ is the river mean water depth (asterisk denotes dimensional quantities). This scaling is adopted for all the vertical lengths so that the stochastically varying river free surface position, h, has null average value and min $[h] = -1$ (see Figure 1c). The biomass is normalized with the maximum carrying capacity, v^*_{max}, that is the species-specific biomass that a riparian plot can sustain, when the phreatic surface is constant at the depth δ_{opt}. It follows that $v = [0, 1]$.

Equation (1) allows an analytical solution of the stochastic dynamics, i.e., the plot-dependent probability density function of v in a closed form. Nevertheless, this relation is not simplistic. It captures the positive correlation between vegetation and bed elevation that is not fixed (as in previous analytical models) but fluctuates, following rigidly the dynamics of v. The topographic alterations are considered instantaneous, as sedimentation/erosion processes exhibit a hourly timescale, while riparian vegetation and discharge typically have timescales of order of tens of day. Furthermore, (1) can be interpreted as a first-order approximation of more general functions $\Delta\eta = f(v)$. As $v \leq 1$, the higher-order terms have a weak effect compared to the first-order term.

The vegetation-induced bed elevation changes impact strongly on the dynamics of the vegetation. The decay/growth switching does depend not only on the stochastic water stage fluctuations and on the plot elevation but also on the vegetation biomass. The vegetation can increase the plot elevation to an extent proportional to its biomass, thus reducing the risk of being flooded and the magnitude of the flood-related damages. Therefore, vegetation is no longer considered a passive element with dynamics driven by an external stochastic forcing. By contrast, it is considered to actively modify the system to its own advantage.

At a generic plot of coordinate x of the river transect (see Figure 1c) the physical processes previously described can be modeled by the piecewise dimensionless equations

$$\frac{dv}{dt} = \begin{cases} -\alpha_1 v^n & h \geq \eta_0 + \Delta\eta(v) \\ v^m (V_{cc} - v)^p & h < \eta_0 + \Delta\eta(v), \end{cases} \tag{2}$$

where $t = t^* \cdot \alpha_2$ is time (α_2 is the species-specific growth rate), $\alpha_1 = (K/\alpha_2)(h - \eta) = k(h - \eta)$ is the vegetation decay rate proportional to the water depth (K is a species-specific coefficient that quantifies the vegetation tolerance to floods), V_{cc} is the plot-specific carrying capacity, and m, n, p are exponents that account for possible nonlinearities in the growth/decay mechanisms. Equation (2a) describes the decay of vegetation biomass induced by anoxia, uprooting, and burial, occurring when the plot is flooded (i.e., $h \geq \eta$). By contrast, (2b) models the vegetation growth occurring when the plot is exposed (i.e., $h < \eta$). Notice that the vegetation and the vegetation-induced topographic alterations are assumed not to modify the rating curve of the river section. Moreover, (2) describes the 1-D dynamics of vegetation along a single transect, and the analysis of 2-D vegetated patterns requires a more sophisticated approach [*Crouzy et al.*, 2015]. The dimensionless carrying capacity is expressed as $V_{cc} = 1 - a(\delta - \delta_{opt})^2$ if $\delta_1 \leq \delta \leq \delta_2$ and zero otherwise, where the depth of the phreatic surface reads $\delta = \eta_0 - h$ [*Camporeale and Ridolfi*, 2006]. The two key characteristics of the approach are (i) the stochasticity of model (2), with the decay rate, the carrying capacity, and the switching between equations forced by the random variable, h, and (ii) the switching between phases of growth and decay depends on if $\eta(v) \gtrless h$; i.e., it is state dependent, as it depends on the system variable, v. This last point makes the present model mathematically more complex than the original one by *Camporeale and Ridolfi* [2006], which can be restored if $r = 0$. For the sake of simplicity, in the following we will set $m = n = p = 1$, but any extension is straightforward.

3. Analytical Solution

To solve the stochastic model (2), the average rate of vegetation decay, α, and the mean carrying capacity, β, are computed [*Camporeale and Ridolfi*, 2006, 2007]. The first rate is evaluated as

$$\alpha = \frac{1}{P_f}\int_{\eta}^{\infty} \alpha_1 p(h)\mathrm{d}h = \frac{1}{P_f}\int_{\eta_0+r\cdot v}^{\infty} k[h-(\eta_0+rv)]p(h)\mathrm{d}h, \tag{3}$$

where $P_f = \int_{\eta_0+r\cdot v}^{\infty} p(h)\mathrm{d}h$ is the probability of being in flooded conditions (i.e., $h > \eta_0 + rv$). Relation (3) highlights the twofold beneficial role of the vegetation-induced morphological changes (i.e., $rv > 0$). It increases the threshold water stage above which the vegetation is damaged and reduces the damage inflicted by the water level, h, that is proportional to $(h-\eta_0-rv)$ and not to $(h-\eta_0)$.

The mean carrying capacity reads

$$\beta = \frac{1}{P_e}\int_{-1}^{\eta} V_{cc}p(h)dh = \frac{1}{P_e}\int_{-1}^{\eta_0+rv} 1 - a(\eta_0 - h - \delta_{opt})^2 p(h)dh, \tag{4}$$

where $P_e = \int_{-1}^{\eta_0+r\cdot v} p(h)\mathrm{d}h$ is the probability of being in exposure conditions.

The average rates, α and β, replace the functions, α_1 and V_{cc}, in the model (2) so that two new functions, $f_f(v) = -\alpha v$ and $f_e(v) = v(\beta - v)$, are obtained. These functions describe the vegetation dynamics in flooded and exposure conditions and determine the overall vegetation dynamics, by switching randomly. This stochastic problem falls in the class of state-dependent dichotomous Markov noises [*Ridolfi et al.*, 2011]. For this type of problems the steady state probability density function (pdf) was recently given in the closed form

$$p(v) = C\left[\frac{1}{f_f(v)} - \frac{1}{f_e(v)}\right]\exp\left\{-\int_v\left[\frac{1}{T_f(v')f_f(v')} - \frac{1}{T_e(v')f_e(v')}\right]\mathrm{d}v'\right\}, \tag{5}$$

where C is a normalization constant so that $\int_0^{\infty} p(v)\mathrm{d}v = 1$ and $T_e(v)$ and $T_f(v)$ are the average durations of the flooded and exposure periods at the plot, respectively.

Equations (3)–(5) are valid for any probability distribution of the water stage, $p(h)$. A common choice [*Doulatyari et al.*, 2014] is to model water stage time series as a random sequence of exponentially distributed jumps (i.e., a white shot noise) and exponential decay. In this case, $p(h)$ is the Gamma distribution

$$p(h) = \frac{\lambda^{\lambda} e^{-(h+1)\lambda}(h+1)^{\lambda-1}}{\Gamma[\lambda]}, \tag{6}$$

where $\lambda = 1/C_h^2$ (C_h is the coefficient of variation of the water levels) and $\Gamma[\cdot]$ is the Gamma function [*Abramowitz and Stegun*, 1964]. $T_e(v)$ can be analytically evaluated as the mean first passage time between two flooding events [*Laio et al.*, 2001], while it can be demonstrated that $T_f(v) = T_e(v)P_f(v)/P_e(v)$. The values of α and β can be obtained in closed form through a formal expansion in Taylor series in the parameter r around η_0. In this way, the integral appearing in (5) reads

$$p(v) = Cv^{c_0}(T_{eL})^{c_1}(T_{eL})^{c_2}(\alpha_L)^{c_3}(\beta_L - v)^{c_4}(\alpha_L + \beta_L - v). \tag{7}$$

The expressions $T_{eL}, T_{fL}, \alpha_L, \beta_L$ as well as the exponents $c_0 - c_4$ are listed in the supporting information. Equation (7) gives the pdf of the biomass of the riparian vegetation as a function of the vegetation type, position of the plot in the river transect, and the probability structure of the river water stage.

4. Results About the Cooperative Dynamics

4.1. General Behaviors

In order to explore the interplay between flow-induced stochasticity, vegetation, and morphology, typical hydrological and biomorphological characteristics are considered. Figures 2a and 2b show the spatial behavior along the river transect of the mean, μ, and standard deviation, σ, of the vegetation biomass distribution, $p(v)$. Four values of the coupling coefficient, r, appearing in equation (1) are considered. For the sake of simplicity, the transverse coordinate is made dimensionless so that $x = \eta$.

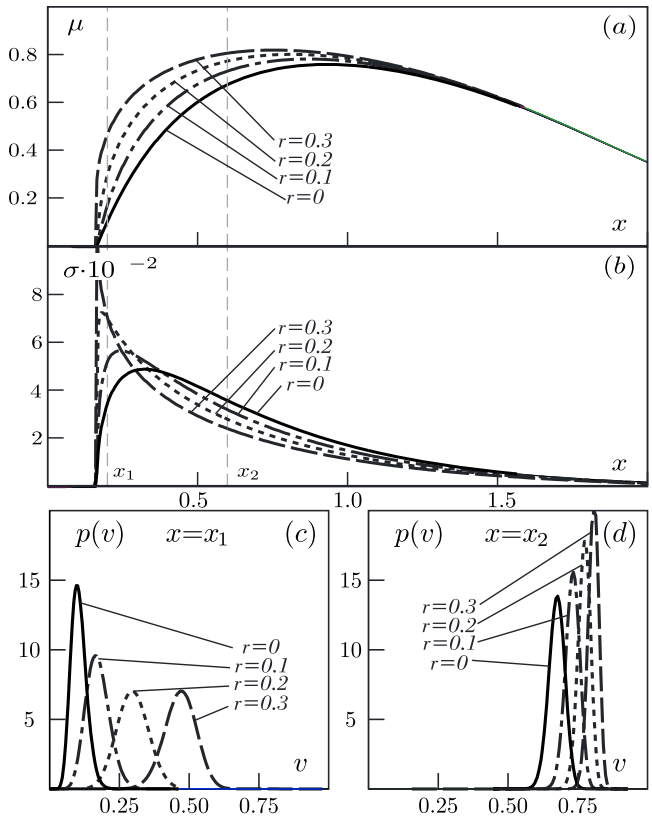

Figure 2. (a) The mean value, μ, and (b) the standard deviation, σ, of the riparian vegetation distribution, $p(v)$, along the transect for different values of r. (c, d) The riparian vegetation distribution, $p(v)$, calculated at $x_1 = 0.2$ and $x_2 = 0.6$, respectively with $\{C_h, \delta_{opt}, \tau, a, k\} = \{0.5, 0.25, 0.01, 0.2, 5\}$.

The mean value behaves differently in two distinct regions: for low sites ($x \lesssim 1.0$), μ increases significantly with r. For higher sites the interplay between vegetation and morphology is negligible. Close to the river the limiting factor is the occurrence of floods, which periodically damage the vegetation. The flood-induced biomass loss is proportional to the flood magnitude, as the bed shear stress scales with the water depth of the plot. Whenever the vegetation biomass increases, the bed elevation rises, the effects of flood is reduced, and an increment of biomass is promoted. This increment is high at lower plots, where the flood-induced damages are more severe and the protection offered by an elevation increment is more impacting. For example, Figure 2c reports $p(v)$ evaluated for different values of r at a point close to the river and shows that the biomass switches from $v \sim 0.1$ for $r = 0$ to $v \sim 0.5$ for $r = 0.3$. Figure 2d refers to a plot further from the river, and the increment of biomass appears progressively reduced. In fact, far from the river the limiting factor is the water availability of the phreatic aquifer. Any sediment deposition protects the vegetation in case of extreme floods but has no effect on the groundwater tapping. Far from the river mean stage (i.e., $x \gg 1$), the average biomass is not affected by the morphology-mediated mechanism of vegetation self-protection.

Figure 2b depicts two distinct behaviors of σ along the river transect. For low sites ($x \lesssim 0.5$, in this case), the coupling between vegetation and morphology induces a strong increment of σ, while for high x a mild reduction of the biomass standard deviation with respect to the parameter r is observed. The vegetation-induced bed increments can protect vegetation from weak floods, but intense inundations cause anyway strong damages. At plots with elevation around the river mean stage (i.e., $x = 0$) both weak and strong inundations take place. The vegetation-induced bed increment protects the vegetation against weak floods and is sufficient to induce an increment of the mean biomass. Strong floods that damage the vegetation (i.e., reduce the biomass) also occur. It follows that an increment in the temporal variability of v is observed, with respect to the case without the coupling (i.e., $r = 0$). For example, the pdfs reported in Figure 2c show that the mean biomass is $\mu \sim 0.45$, for $r = 0.3$. It is not unlikely to have biomass as low (high) as 0.3 (0.6). Moving away from the river, the probability of inundation decreases. Sediment aggradation further reduces this probability, and

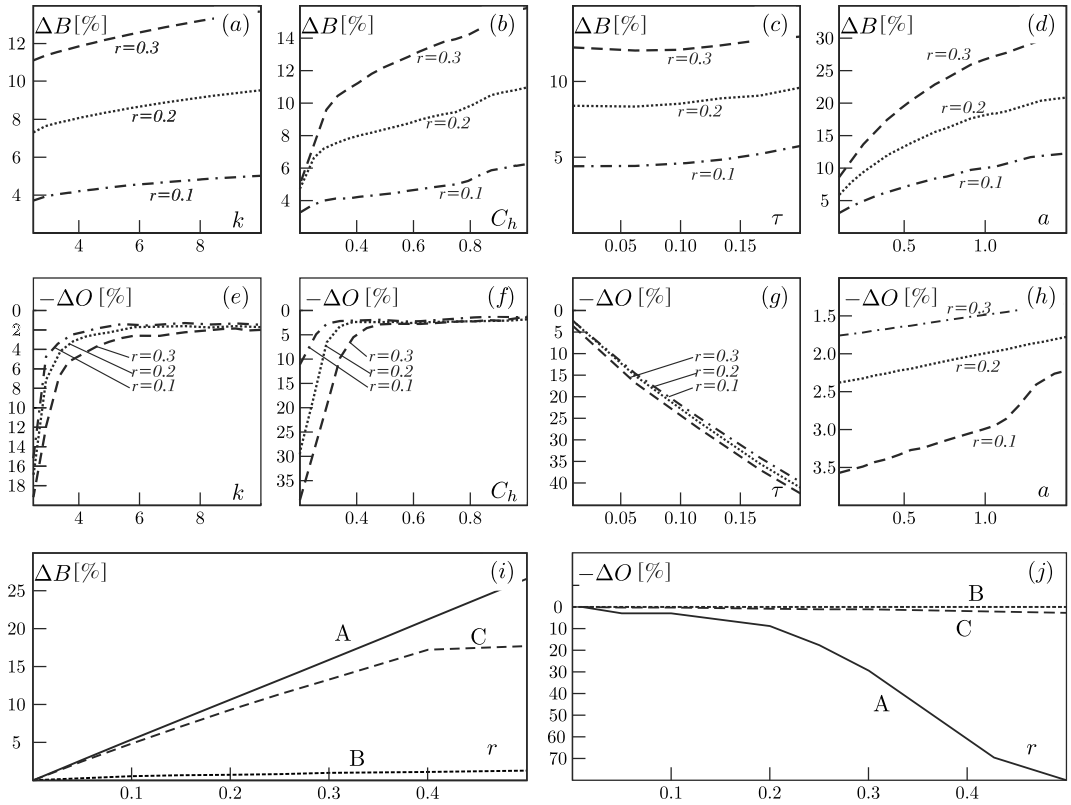

Figure 3. (a–h) Sensitivity analysis of the main modeling parameters, where only one parameter at time is changed with respect to the benchmark set $\{C_h, \tau, a, k, \delta_{opt}\} = \{0.5, 0.01, 0.2, 5, 0.25\}$. The effects on the increment of mean biomass along the transect, ΔB, are reported in Figures 3a–3d and the effects on the displacement of the vegetated zone, ΔO, are in Figures 3e–3h. (i–j) The effects of the coupling coefficient r on ΔB and ΔO, respectively, for three idealized cases: A, $\{C_h, k\} = \{0.6, 6\}$; B, $\{C_h, k\} = \{0.4, 4\}$; and C, $\{C_h, k\} = \{0.2, 2\}$.

the damages caused by inundations as well. It follows that the biomass tends to the local carrying capacity (that decreases due to groundwater deepening), and the standard deviation approaches to zero (Figure 2d).

In order to investigate the beneficial impact of the vegetation-morphology feedback on vegetation, the increment of mean biomass along the transect, ΔB, and the displacement of the vegetated zone, ΔO, are defined. The first metric is $\Delta B := B_r/B_0 - 1$, where $B = \int_0^{\infty} \mu(x) dx$ is the total mean biomass along the river transect and the subscripts refer to the value of the coupling coefficient, r. The second metric reads $\Delta O := O_r/O_0 - 1$, where O is the elevation of the closest point to the river where the mean biomass is larger than 0.01 (here conventionally assumed as the starting point of the vegetated zone). Figure 3 reports ΔB and ΔO as a function of the most important hydrological and biological parameters. In order to explore different magnitude of the vegetation feedback on the topography, three values of the coupling coefficient $r = (0.1, 0.2, 0.3)$ are considered.

Figure 3 shows that the increment of biomass, ΔB, is always significant. It ranges from 4–5% to 15–30%, depending on the parameter set. The extent of the consequences of the feedback between vegetation and topography depends on the river and vegetation characteristics. In particular, the consequences are more pronounced when (i) the vegetation is fragile to inundations, namely high values of k occur (Figure 3a); (ii) the river stage fluctuations around the mean level are high; i.e., C_h is high (Figure 3b); and (iii) the optimal depth interval $[\delta_1, \delta_2]$ of the phreatic surface becomes narrower; i.e., a is high (Figure 3d). Finally, the river stage correlation time has a negligible effect on the increase in the biomass (Figure 3c) as already pointed out by *Camporeale and Ridolfi* [2006].

The plots far from the river can be colonized by vegetation even without the occurrence of the vegetation-induced bed elevation increment (i.e., the case $r = 0$). In these plots, the consequence of the feedback is to increase the mean value of biomass. Moreover, in some plots close to the river, the feedback allows also a colonization that would have been impossible otherwise. If the vegetation-induced increment of bed

elevation had not been occurred, in those plots the vegetation would have been completely removed during any flood. As a result, those plots would have been bare. The capability of vegetation to increase its plot elevation induces a shifting of the vegetated front, with a planimetric extent that depends on the lateral slope of the transect. The front shifting is registered by the behavior of ΔO. Figures 3e and 3f show a remarkable stream narrowing occurring when flood-resistant vegetation (k small) or regular river flows (C_h small) are considered. In both cases, the vegetation-induced aggradation of plot is decisive for the shifting of the vegetated front.

Although the river stage correlation time has a marginal role on the total biomass, it significantly affects the quantity O_r (Figure 3g). When time correlation, τ, is high, long periods of plot exposure and inundation alternate. During exposures, the vegetation has enough time to grow and to induce a significant increment of the plot elevation. As a result, the protection of the plot against successive floods is increased, and the vegetation can colonize other sites closer to the river.

The impact of the coefficient r on ΔB and ΔO is reported for three emblematic cases in Figures 3i and 3j, in order to highlight the benefit on vegetation resulting from the coupling between biological and morphological processes. In the case A, vegetation is sensitive to inundations, and the river water stage exhibits large fluctuations ($\{C_h, k\} = \{0.6, 6\}$). In the case B, vegetation is weakly sensitive to inundations and the river fluctuations are small ($\{k, C_h\} = \{2, 0.2\}$). The case C has intermediate values ($\{k, C_h\} = \{4, 0.4\}$).

In the case A, the vegetation takes advantage from the vegetation-induced morphological alterations. When the coupling is high ($r = 0.5$), the biomass increases up to 25%, and the first vegetated plot gets closer to the river by 70%. Also, if the coupling is weak (e.g., $r = 0.2$; see Figure 3i) significant benefits are attained ($\Delta B \sim 10\%$, $\Delta O \sim -20\%$). A completely different behavior is observed in case B. Although the vegetation can induce consistent sediment deposition when $r = 0.5$, the biomass increment and the migration of the first vegetated plot are less than 1%. The riparian vegetation is so flood resistant, and the water stage variations are so weak that the rise of elevation induced by vegetation has no consequences on the vegetation. Finally, the case C shows that for $r \sim 0.4$ a threshold value r_c occurs, in the case reported in the figure. At $r < r_c$ the increment of biomass is relevant and increases proportionally to the coupling strength (similarly to the case A). At $r > r_c$, ΔB becomes a constant; i.e., no additional benefits are gained by the vegetation in spite of its ability to increase further the plot elevation. This behavior suggests that the cooperation between vegetation and morphology is efficient up to a threshold. The exact value of this threshold depends on the interplay between the stochastic hydrological features of the river and the vegetation properties. In the cases A and B, this limit corresponds to very high and low values of r, respectively, while it falls on intermediate values in the case C.

4.2. Field Case

Some field observations about the riparian vegetation dynamics along the Tagliamento river are now discussed. In particular, the elevation of the lowest vegetated point of some specific reaches of the Tagliamento braided network can be derived from the data reported by *Bertoldi et al.* [2011]. For instance, in the Flagogna reach (Figures 1a and 1b), no vegetation taller than 1 m has been found below $\eta^*_{\min} \sim 0.5$ m (where the datum $\eta^* = 0$ corresponds to the lowest point of the reach bed). Moreover, the same authors detected that a Gamma distribution captures the distribution of the bed elevation in the considered reach.

The water stage time series of the Tagliamento at the Venzone gauging station, 8 km upstream of the Flagogna reach, is also available (from hydrographic office of Venezia-Giulia). The relationship between the overall width of the active channels, W^*, and the discharge, Q^*, is given by $W^* = 23.8 Q^{*0.52}$ [*Welber et al.*, 2012]. With this information and by adopting the hydrogeomorphologic procedure reported in the additional material, one can obtain the mean ($\bar{h}^* = 0.35$ m), the coefficient of variation ($C_h = 0.25$), and the integral scale (35 days) of the water stage time series.

The Flagogna reach mainly hosts *Populus nigra* and several willow species [*Bertoldi et al.*, 2011]. Therefore, it is reasonable to assume for the biotic parameters the standard values $\{a, \delta_{opt}, \alpha_2\} \simeq \{0.22, 2.5\text{m}, 10^{-4}\text{d}^{-1}\}$ [*Young et al.*, 1980]. Accordingly, $\tau = \alpha_2 \tau^* = 0.0035$. Finally, $k = 10$ and $r = 0.1$ are assumed, in order to consider a moderate feedback between the vegetation and plot elevation. With this setting, the present stochastic model estimates that the vegetation onset occurs at $\eta^* = 0.45$ m, which is in good agreement with the field observation by *Bertoldi et al.* [2011]. A sensitivity analysis with $\pm 20\%$ of model parameters (parameters were changed one at a time) was used to check the robustness of the obtained result. The obtained values of η^* are in the range [0.43, 0.50] m.

5. Conclusions

A novel state-dependent stochastic model is proposed for describing the cooperation between vegetation and topography in environments forced by random water stage fluctuations. This cooperation is based on a fundamental positive feedback. The vegetation induces bed aggradation; the probability of flooding is therefore reduced, and this is a benefit for the vegetation itself. These mechanisms make evident how biotic/abiotic and deterministic/stochastic processes are closely linked in the river environments, concur to generate complex dynamical equilibria, and are of paramount importance to understand large-scale man-induced catastrophic shifts of river systems. The minimalistic stochastic approach can be therefore a suitable method for obtaining analytical results useful for the management of rive landscapes.

Notation

C_h coefficient of variation of the river stage;
τ correlation time of the river stage;
k vegetation sensitivity to flooding conditions;
δ_{opt} phreatic surface depth for the optimal plant growth;
a sensitivity of vegetation to the departure of the phreatic surface from its optimal position;
$p(v)$ plot-specific pdf of the vegetation biomass;
μ plot-specific mean value of $p(v)$;
σ plot-specific standard deviation of $p(v)$;
ΔB relative increment (in percentage) of mean biomass along the transect;
ΔO relative displacement (in percentage) of the vegetated front.

Acknowledgments
Data will be provided upon request.

The Editor thanks two anonymous reviewers for their assistance in evaluating this paper.

References

Abbe, T., and D. Montgomery (2003), Patterns and processes of wood debris accumulation in the Queets river basin, Washington, *Geomorphology*, *51*(1–3), 81–107.

Abramowitz, M., and I. Stegun (1964), *Handbook of Mathematical Functions: With Formulas, Graphs, and Mathematical Tables*, Dover, New York.

Bennett, S. J., W. Wu, C. V. Alonso, and S. S. Y. Wang (2008), Modeling fluvial response to in-stream woody vegetation: Implications for stream corridor restoration, *Earth Surf. Processes Landforms*, *33*(6), 890–909.

Bertoldi, W., A. M. Gurnell, and N. A. Drake (2011), The topographic signature of vegetation development along a braided river: Results of a combined analysis of airborne lidar, color air photographs, and ground measurements, *Water Resour. Res.*, *47*, W06525, doi:10.1029/2010WR010319.

Bertoldi, W., A. Siviglia, S. Tettamanti, M. Toffolon, D. Vetsch, and S. Francalanci (2014), Modeling vegetation controls on fluvial morphological trajectories, *Geophys. Res. Lett.*, *41*, 7167–7175, doi:10.1002/2014GL061666.

Beschta, R. L., and W. J. Ripple (2006), River channel dynamics following extirpation of wolves in northwestern Yellowstone National Park, USA, *Earth Surf. Processes Landforms*, *31*(12), 1525–1539, doi:10.1002/esp.1362.

Camporeale, C., and L. Ridolfi (2006), Riparian vegetation distribution induced by river flow variability: A stochastic approach, *Water Resour. Res.*, *42*, W10415, doi:10.1029/2006WR004933.

Camporeale, C., and L. Ridolfi (2007), Noise-induced phenomena in riparian vegetation dynamics, *Geophys. Res. Lett.*, *34*, L18406, doi:10.1029/2007GL030899.

Camporeale, C., E. Perucca, L. Ridolfi, and A. M. Gurnell (2013), Modeling the interactions between river morphodynamics and riparian vegetation, *Rev. Geophys.*, *51*, 379–414, doi:10.1002/rog.20014.

Corenblit, D., E. Tabacchi, J. Steiger, and A. M. Gurnell (2007), Reciprocal interactions and adjustments between fluvial landforms and vegetation dynamics in river corridors: A review of complementary approaches, *Earth Sci. Rev.*, *84*(1–2), 56–86.

Craig, L. S., et al. (2008), Stream restoration strategies for reducing river nitrogen loads, *Front. Ecol. Environ.*, *6*(10), 529–538.

Crosato, A., and M. S. Saleh (2011), Numerical study on the effects of floodplain vegetation on river planform style, *Earth Surf. Processes Landforms*, *36*(6), 711–720.

Crouzy, B., F. Brenbold, P. D'Odorico, and P. Perona (2015), Ecomorphodynamic approaches to river anabranching patterns, *Adv. Water Res.*, doi:10.1016/j.advwatres.2015.07.011.

Docker, B. B., and T. C. T. Hubble (2008), Quantifying root-reinforcement of river bank soils by four Australian tree species, *Geomorphology*, *100*(3–4), 401–418.

D'Odorico, P., F. Laio, A. Porporato, L. Ridolfi, and N. Barbier (2007), Noise-induced vegetation patterns in fire-prone savannas, *J. Geophys. Res.*, *112*, G02021, doi:10.1029/2006JG000261.

Doulatyari, B., S. Basso, M. Schirmer, and G. Botter (2014), River flow regimes and vegetation dynamics along a river transect, *Adv. Water Res.*, *73*, 30–43.

Gibling, M. R., and N. S. Davies (2012), Palaeozoic landscapes shaped by plant evolution, *Nat. Geosci.*, *5*(2), 99–105, doi:10.1038/NGEO1376.

Gurnell, A. (2014), Plants as river system engineers, *Earth Surf. Processes Landforms*, *39*(1), 4–25.

Gurnell, A., K. Tockner, P. Edwards, and G. Petts (2005), Effects of deposited wood on biocomplexity of river corridors, *Front. Ecol. Environ.*, *3*(7), 377–382.

Gurnell, A. M., W. Bertoldi, and D. Corenblit (2012), Changing river channels: The roles of hydrological processes, plants and pioneer fluvial landforms in humid temperate, mixed load, gravel bed rivers, *Earth Sci. Rev.*, *111*(1–2), 129–141.

Hickin, E. (1984), Vegetation and river channel dynamics, *Can. Geogr. Geogr. Can.*, *28*(2), 111–126.

Ishikawa, Y., T. Sakamoto, and K. Mizuhara (2003), Effect of density of riparian vegetation on effective tractive force, *J. For. Res.*, *8*(4), 235–246.
Jones, C., J. H. Lawton, and M. Shachak (1994), Organisms as ecosystem engineers, *Oikos*, *69*(3), 373–386, doi:10.2307/3545850.
Kozlowski, T. (1984), Responses of woody plants to flooding, in *Flooding and Plant Growth*, edited by T. Kozlowski, pp. 129–163, Physiological Ecology, Academic Press, Orlando, Fla.
Laio, F., A. Porporato, L. Ridolfi, and I. Rodriguez-Iturbe (2001), Mean first passage times of processes driven by white shot noise, *Phys. Rev. E*, *63*, 036105.
Malanson, G. (1993), *Riparian Landscapes*, Cambridge Univ. Press, Cambridge.
Marani, M., C. Da Lio, and A. D'Alpaos (2013), Vegetation engineers marsh morphology through multiple competing stable states, *Proc. Natl. Acad. Sci. U.S.A.*, *110*(9), 3259–3263.
Muneepeerakul, R., A. Rinaldo, and I. Rodriguez-Iturbe (2007), Effects of river flow scaling properties on riparian width and vegetation biomass, *Water Resour. Res.*, *43*, W12406, doi:10.1029/2007WR006100.
Naiman, R., H. Décamps, and M. McClain (2005), *Riparia*, Elsevier Academic, Burlington.
Naumburg, E., R. Mata-Gonzalez, R. G. Hunter, T. Mclendon, and D. W. Martin (2005), Phreatophytic vegetation and groundwater fluctuations: A review of current research and application of ecosystem response modeling with an emphasis on great basin vegetation, *Environ. Manage.*, *35*(6), 726–740.
Nicholas, A. P., P. J. Ashworth, G. H. S. Smith, and S. D. Sandbach (2013), Numerical simulation of bar and island morphodynamics in anabranching megarivers, *J. Geophys. Res. Earth Surf.*, *118*, 2019–2044, doi:10.1002/jgrf.20132.
Pasquale, N., P. Perona, R. Francis, and P. Burlando (2012), Effects of streamflow variability on the vertical root density distribution of willow cutting experiments, *Ecol. Eng.*, *40*, 167–172.
Ridolfi, L., P. D'Odorico, and F. Laio (2011), *Noise-Induced Phenomena in the Environmental Sciences*, Cambridge Univ. Press, Cambridge.
Shafroth, P., J. Stromberg, and D. Patten (2002), Riparian vegetation response to altered disturbance and stress regimes, *Ecol. Appl.*, *12*(1), 107–123.
Steiger, J., A. Gurnell, P. Ergenzinger, and D. Snelder (2001), Sedimentation in the riparian zone of an incising river, *Earth Surf. Processes Landforms*, *26*(1), 91–108.
Tealdi, S., C. Camporeale, and L. Ridolfi (2011), Modeling the impact of river damming on riparian vegetation, *J. Hydrol.*, *396*(3–4), 302–312.
Tockner, K., F. Malard, and J. Ward (2000), An extension of the flood pulse concept, *Hydrol. Processes*, *14*(16-17), 2861–2883.
Welber, M., W. Bertoldi, and M. Tubino (2012), The response of braided planform configuration to flow variations, bed reworking and vegetation: The case of the Tagliamento River, Italy, *Earth Surf. Processes Landforms*, *37*(5), 572–582.
Wu, W., F. Shields, S. Bennett, and S. Wang (2005), A depth-averaged two-dimensional model for flow, sediment transport, and bed topography in curved channels with riparian vegetation, *Water Resour. Res.*, *41*, W03015, doi:10.1029/2004WR003730.
Young, H. E., J. H. Ribe, and K. Wainwright (1980), Weight tables for tree and shrub species in Maine, Tech. Rep., Univ. of Maine, Orono.